  Bull. Chem. Soc. Jpn., 56, 2093—2100 (1983)

The Heat Capacities of Lithium, Sodium, Potassium, Rubidium, and Caesium Nitrates in the Solid and Liquid States

Kazuhiko Ichikawa* and Toshiyuki Matsumoto

Department of Chemistry, Faculty of Science, Hokkaido University, Sapporo 060

(Received December 24, 1982)

The heat capacities, C_p, of the alkali metal nitrates, MNO_3 (M=Li, Na, K, Rb, and Cs), in the solid and liquid states have been measured between 50 and 450 °C by means of adiabatic calorimetry. We have measured with a fair degree of accuracy the C_p values for the MNO_3 systems, because the existing data on $NaNO_3$ and KNO_3 above 250 °C are quite scanty. Some empirical rules, some of which may extend to other salts, have been obtained from the results on C_p for the five alkali nitrates in the solid and liquid states. For the molten MNO_3, the heat capacities at a constant volume, C_V, were obtained from the thermodynamical relationship between C_V and C_p, using the experimental values of C_p; the C_V values have been interpreted in terms of the interionic and intraionic portions.

It has become a common theme of research to develop technology for the storage of thermal energy and for heat transfer, employing molten salts; the study of their thermal properties has thus acquired a practical meaning. The salt of most interest is molten alkali-metal nitrate, for it has better physical and chemical properties than other salts. Some of these properties are its low melting point, t_{mp}, its nonvolatile, nondecomposite, and noncorrosive characteristics, and its high heat capacity. The existing data on the heat capacity at constant pressure C_p, for $NaNO_3$ and KNO_3, which were obtained from the slopes of the curves of the heat content *versus* temperature,[1] are quite scanty, in particular just below and above t_{mp}. The thermal property[2] of most interest in this paper is the heat capacity as an important parameter. This work describes briefly an adiabatic calorimeter used to measure high-temperature heat capacities with a fair degree of accuracy (2.0%). The C_p results are shown for the five alkali-metal nitrates MNO_3 (M= Li, Na, K, Rb, and Cs) in the solid and liquid states between 50 and 450 °C. Their heat-capacity data have given rise to some empirical rules, which may extend to other salts. The high heat-capacities observed will also be discussed in terms of their interionic and intraionic contributions.

Experimental

Materials. The salts used were pure-grade recrystallized reagents. The KNO_3 was supplied by Prof. G. J. Janz, Rensselaer Polytechnic Institute, and the $NaNO_3$ and $LiNO_3$ of a special grade, by Wako. The purity of the $RbNO_3$ and $CsNO_3$ purchased from Alfa was 99.9%. Metallic impurities indicated: for KNO_3, Si 0.1—0.5, Mg 0.1—0.5, Fe 0.1—0.5, and Ca 0.5—2.0 ppm; for $NaNO_3$, Pb 0.007, K 0.008, Cu 0.002, Fe 0.003 mass percentage; for $LiNO_3$, Pb 0.001, Na 0.05, K 0.05, Cu 0.0005, Mg 0.005, Ca 0.01, Ba 0.001, Fe 0.005 mass percentage.

Apparatus and Procedure. Measurements of the high-temperature heat capacity, C_p, were made with an adiabatic calorimeter. The adiabatic shield control consists of a PID-SCR circuit, a constant wattage supply, a heater of platinum-wire, and multi-junction thermocouples. The temperature difference between the sample in a calorimetric ampoule (*i.e.*, a platinum cylindrical vessel of *ca.* 7.5 cm^3) and the adiabatic shield was controlled within 0.1 °C between 50 and 450 °C. Since the heat emissivity of the gold metal is very small, the inner adiabatic jacket and the outer vessel of the sample container are gold-plated. The adiabatic calorimeter may be sufficiently protected from the heat leakage due to thermal radiation. In order to get avoid any oxidation and corrosion of the interior of the calorimeter over the entire temperature range of this work, heat-capacity measurements were made under Ar gas of *ca.* 2.5×10^4 Pa at room temperature introduced into the vacuum cell of the calorimeter. The values of C_p in J K^{-1} g^{-1} were computed from the following equation:

$$C_p = (W\cdot\Delta t)/(M\cdot\Delta\theta) - (M'/M)C_p', \quad (1)$$

where W (in watts) is the electric power supplied by the internal heater, Δt (in seconds) is the time required for increasing the temperature by $\Delta\theta$ degrees and is determined by the clock timer unit, and M is the weight (*i.e.*, 10—15 g) of the sample. The heat capacity of the empty calorimeter, $M'C_p'$, was obtained in a preliminary measurement. The temperature measurement was carried out with a Pt-Rh thermocouple calibrated by a cryoscopic method for pure-grade recrystallized reagents, KNO_3, K_2SO_4, Ag_2SO_4, and $KClO_4$.

The experimental errors may originate from two major sources. Firstly, sample characteristics associated with endothermic reactions, such as decomposition and evaporation, should be considered.[3] In this work, however, the weight-loss of the sample between 50 and 450 °C ranged from 0.01% to 0.06%. Thus, the endothermic heat resulting from the decomposition or evaporation of MNO_3 may not affect any magnitudes of C_p within the present experimental uncertainty. Secondly, the calorimeter operation was tested by measuring the C_p of standard synthetic sapphire (99.99 wt% purity). The magnitude of the experimental error

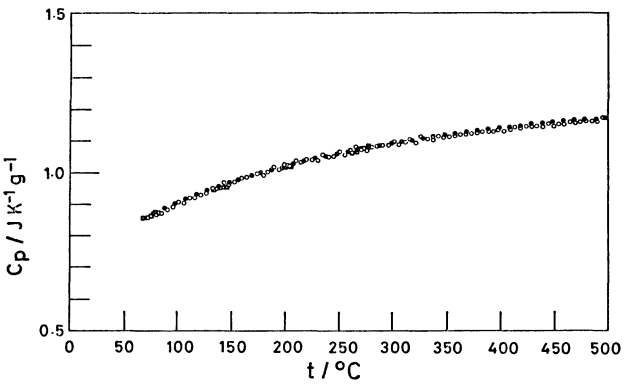

Fig. 1. Temperature dependence of the heat capacity of synthetic sapphire: ○, this work; ●, Ref. 4; □ Ref. 5.

attributable to the heat leakage was less than two per cent of C_p of the sample for the temperatures of interest; Fig. 1 shows that our results of synthetic sapphire agree with the selected values cited in the text published by TPRC[4] and with the existing data, which were measured by a reliable adiabatic calorimeter and which prove the precision to be $\pm 0.3\%$ and give an accuracy of $\pm 0.6\%$.[5] This agreement is sufficient for our present purposes. The amount of argon gas in the interior of the stainless-steel vacuum vessel did not affect the data of C_p within the limits of experimental uncertainty of $\pm 1.0\%$ between 50 and 500 °C.

Results and Discussion

The experimental results on C_p in $J\,K^{-1}\,g^{-1}$ of $LiNO_3$ and $NaNO_3$ between 50 and 400 °C, and of KNO_3, $RbNO_3$, and $CsNO_3$ between 50 and 450 °C are presented in Figs. 2—6 respectively. Their molar heat capacities in $J\,K^{-1}\,mol^{-1}$ are listed in Table 1. It is worthy while focussing on the accuracy of the results, because the literature data are quite scattered above the level of precision of each of the data (*e.g.*, Fig. 3 for $NaNO_3$).[1,6-16]

$NaNO_3$: Figure 3 demonstrates that the many existing data on the C_p of $NaNO_3$ in the solid and liquid states are quite scanty and not in good agreement. Our data are in close agreement with the data of Sokolov and Schmidt,[11] and of Carling[16] except for the neighborhood of the solid-state transition temperature, t_{tr}, which depends on the literature (*i.e.*,

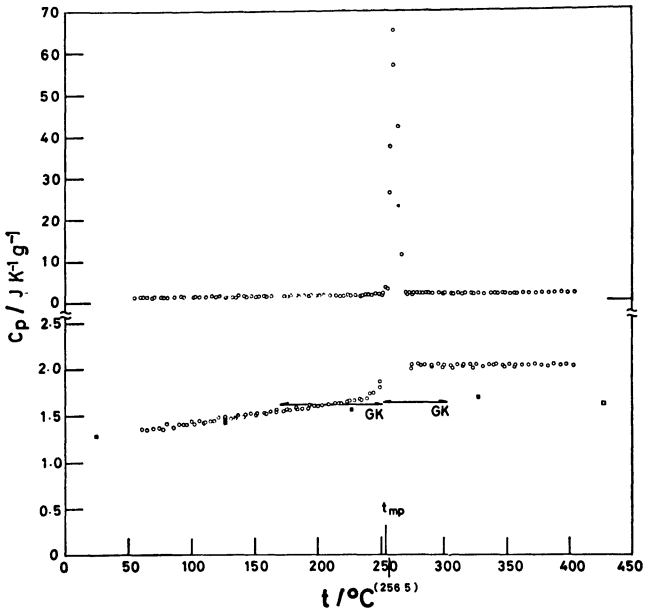

Fig. 2. Temperature dependence of the heat capacity of $LiNO_3$: ○, this work; GK, Ref. 1; ■(solid) and □(liquid), Ref. 21. In this and in Figs. 3—6 the temperatures of t_{tr} and t_{mp} shown by the vertical lines were referred from the literature data and the temperature in parentheses, the location of which is pointed out by an arrow, was determined in this work.

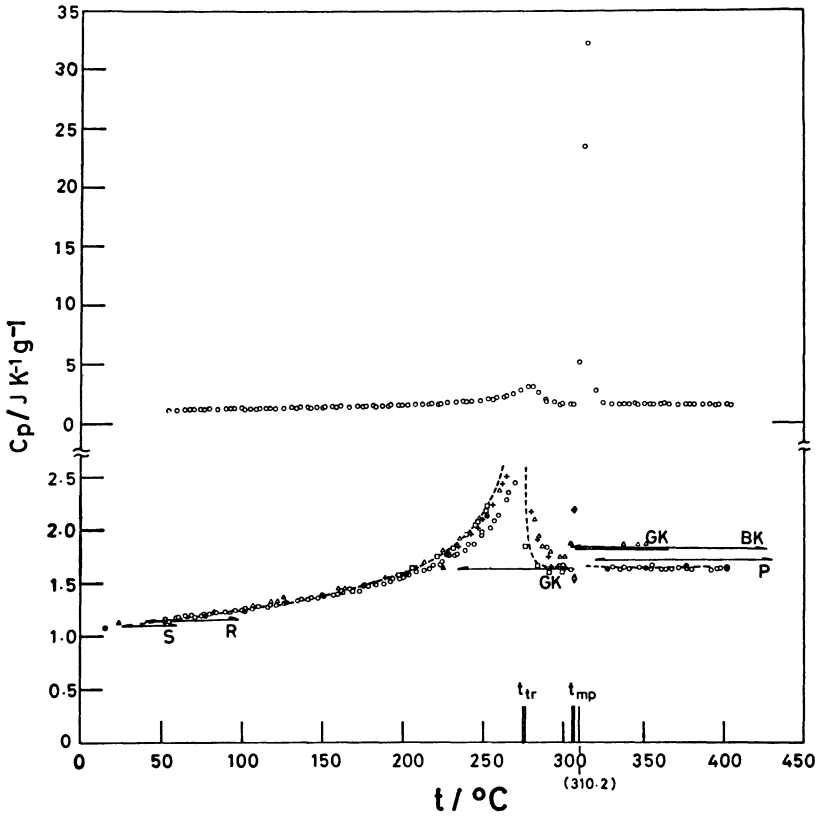

Fig. 3. Temperature dependence of the heat capacity of $NaNO_3$: ○, this work; R, Ref. 6; P, Ref. 7; S, Ref. 8; GK, Ref. 1; ★ Ref. 9; +, Ref. 10; ----, Ref. 11; △, Ref. 12; ◆(solid) and ◇(liquid), Ref. 13; □, Ref. 14; ▲ and BK, Ref. 15; ●, Ref. 16.

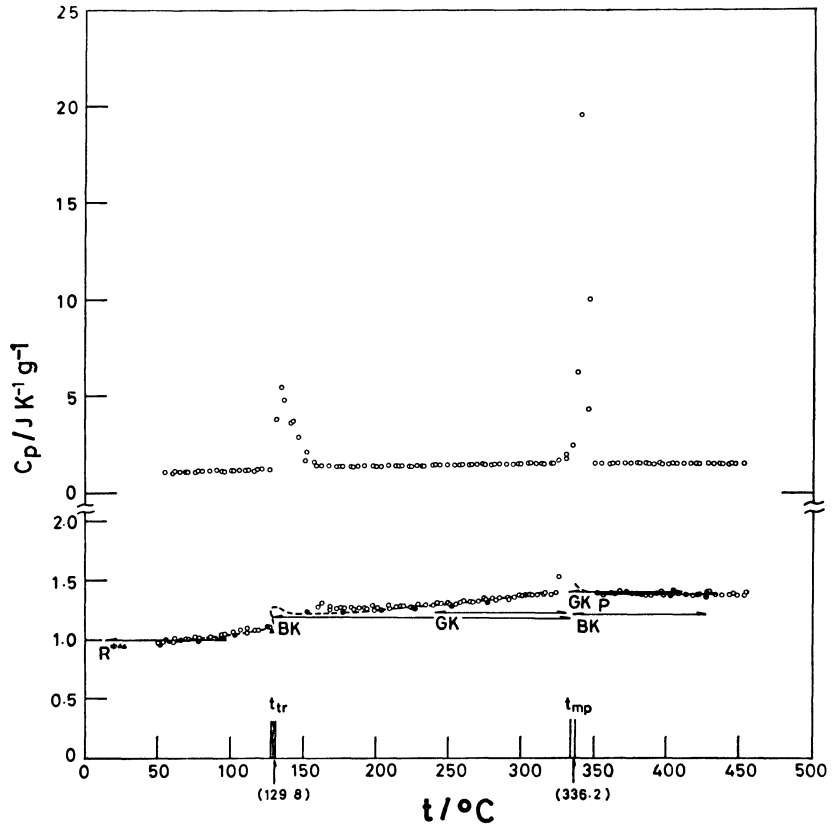

Fig. 4. Temperature dependence of the heat capacity of KNO_3: ○, this work; ----, Ref. 17; the other symbols should be referred in Fig. 3.

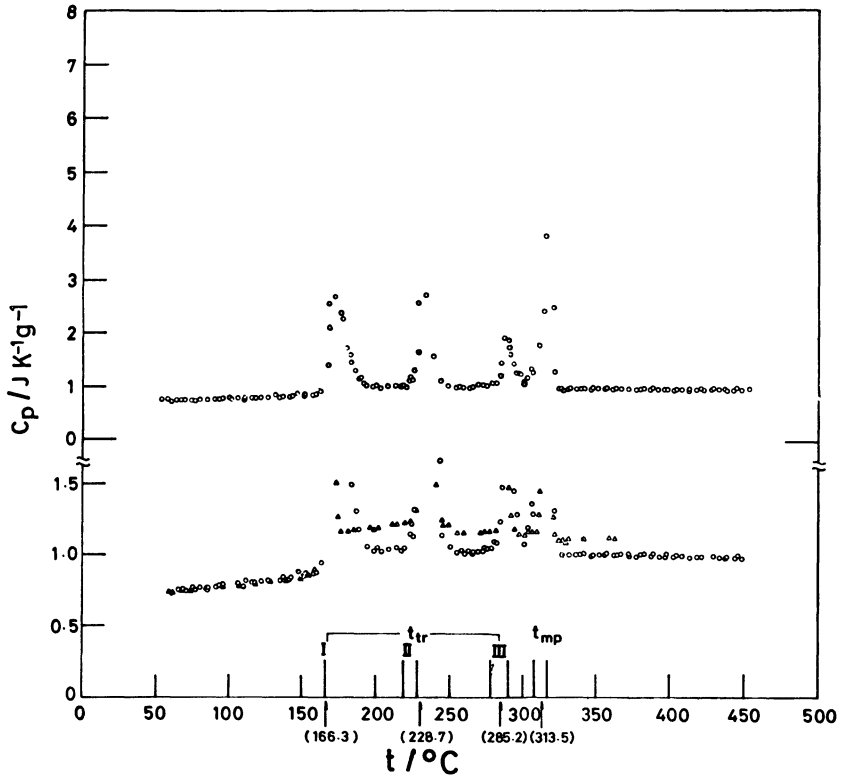

Fig. 5. Temperature dependence of the heat capacity of $RbNO_3$: ○, this work; △, Ref. 19. The three reversible solid-transitions I, II, and III,[33] have been observed and their temperatures and t_{mp} are some what scattered in the literature data.

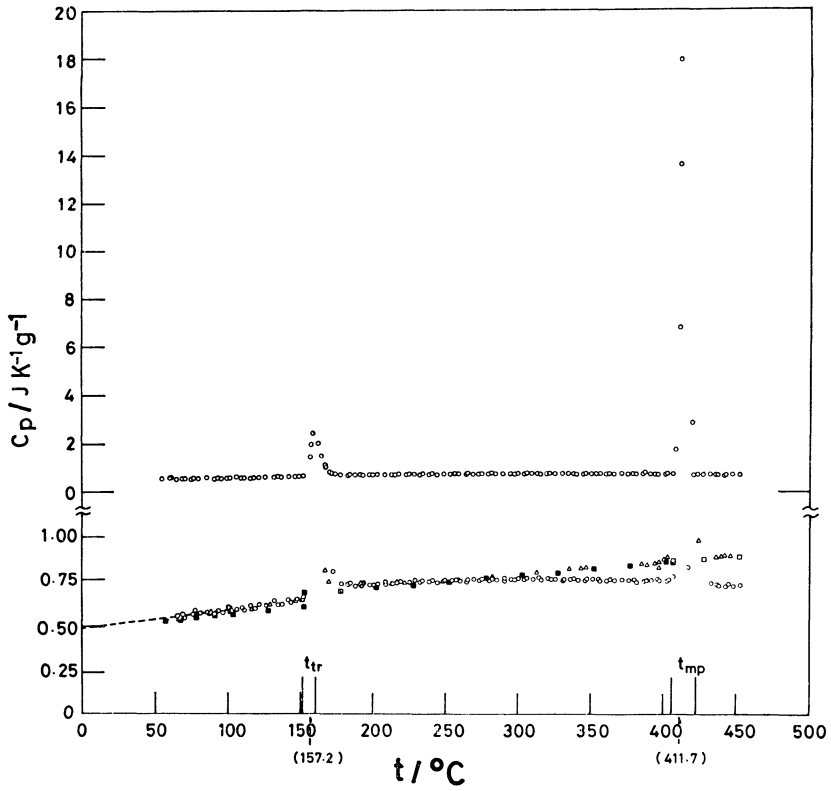

Fig. 6. Temperature dependence of the heat capacity of $CsNO_3$: ○, this work; ----, Ref. 22; △, Ref. 20; ■(solid) and □(liquid), Ref. 23.

275 and 276 °C). Our data also agree with the data of Miekk-oja[10] between t_{tr} and t_{mp}; the data of Reinsborough and Wetmore[14] immediately below t_{mp} are slightly less than ours. On the other hand, Mustajoki's data[12] (for heating) above t_{mp}, which are located above the C_p values (see the horizontal arrows in Fig. 3) obtained from the temperature dependence of enthalpy by Goodwin and Kalmus[1] and by Barir and Knacke,[15] are larger than the data of this work, Sokolov and Schmidt,[11] and Carling[16] by *ca.* 14% above the level of precision of each of the data. It may also be noted that Goodwin and Kalmus'[1] data just below t_{mp} agree satisfactorily with those of this work, Sokolov and Schmidt,[11] and Carling,[16] but the former does not show any broad cusp-shaped peak in the heat capacity curve. The change in the heat capacity on fusion at t_{mp}, $\Delta C_p^\circ(t_{mp})$, is given as the difference between the heat capacities just below t_{mp} and immediately above t_{mp}, wherein the experimental values which show the peak of C_p around the temperature, t_p, located slightly higher than t_{mp} should be omitted. Thus, $\Delta C_p^\circ(t_{mp})$ may be defined by:

$$\Delta C_p^\circ(t_{mp}) \equiv \lim_{\delta\to 0}[C_p^l(t_{mp}+\delta)] - \lim_{\delta'\to 0}[C_p^s(t_{mp}-\delta')], \qquad (2)$$

where the suffixes l and s stand for the liquid and solid states respectively. The mark of $\lim_{\delta \text{ or } \delta'\to 0}$ indicates the extrapolation of C_p until t_{mp}; δ and δ' are positive. Under an ideal condition that both δ and δ' are equal to zero, t_p should be equal to t_{mp}. Figure 3 shows that $\Delta C_p^\circ(t_{mp})$ for $NaNO_3$ is almost zero, as well as KNO_3. On the other hand, $\Delta C_p^\circ(t_{mp})$ in the literature data is either negative or positive (*i.e.*, Goodwin and Kalmus[1]: 15.0 J K^{-1} mol^{-1}, Mustajoki[12]: 3.3, Janz *et al.*[13]: −56.0, Barin and Knacke[15]: −2.6, and Sokolov and Schmidt[11]: 2.9). The magnitude of *ca.* 3 J K^{-1} mol^{-1} is almost comparable with the experimental uncertainty in the C_p values.

KNO_3: There exist data in the literatures which are scattered similar to $NaNO_3$. Our data are in close agreement with the data of Sokolov and Schmidt[17] and of Carling[16] as in the case of $NaNO_3$. Further, our data have reproduced also the data of Person[7] and of Goodwin and Kalmus.[1] To our knowledge there exist no data for KNO_3 above t_{tr} (*i.e.*, the 129.8 °C observed in this work), though Mustajoki[18] reported the data for MNO_3 (M=Na,[12] Rb,[19] and Cs[20]) in the solid and liquid states. In this work, $\Delta C_p^\circ(t_{mp})=0$, and in Carling's data it also seems to be zero, but in the literature data 17.4 J K^{-1} mol^{-1} has been reported by Goodwin and Kalmus[1] and 2.9 by Barin and Knacke.[15] For both $NaNO_3$ and KNO_3, the values extrapolated to room temperature agree well with their heat capacities at the low temperatures measured by Southard and Nelson,[9] as is shown in Figs. 3 and 4.

The magnitudes and the temperature dependence of the C_p values were not determined from the slopes of the curves of the heat content and the corresponding temperatures with sufficient accuracy, for the differences in the C_p values between our data and the data of Goodwin and Kalmus or the data tabulated by Barin and Knacke are dependent on the systems above

TABLE 1. EXPERIMENTAL HEAT CAPACITIES OF ALKALI METAL NITRATES MNO_3 (M=Li, Na, K, Rb, AND Cs) IN THE SOLID AND LIQUID STATES

t / °C	C_p / J K^{-1} mol^{-1}	t / °C	C_p / J K^{-1} mol^{-1}	t / °C	C_p / J K^{-1} mol^{-1}	t / °C	C_p / J K^{-1} mol^{-1}	t / °C	C_p / J K^{-1} mol^{-1}	t / °C	C_p / J K^{-1} mol^{-1}
			$LiNO_3$					Solid-Liquid transition			
59.7	91.6	131.7	101.4	192.2	108.7	351.5	140.8	388.1	139.4	422.7	139.8
60.7	93.6	134.7	101.2	193.2	111.1	355.6	139.6	392.2	139.7	427.8	140.4
64.8	93.4	136.8	104.0	198.3	110.6	361.7	140.4	396.3	141.6	428.8	142.0
70.0	94.1	141.9	103.6	200.3	110.6	363.7	141.1	397.3	139.5	432.9	139.2
75.1	94.5	142.9	104.0	203.4	110.9	371.9	141.4	402.4	139.4	436.9	140.0
77.2	93.8	147.0	104.9	208.5	111.7	371.9	141.6	404.4	140.0	438.0	139.1
85.4	95.4	151.1	104.0	208.5	111.9	377.0	139.8	407.5	140.4	443.0	138.9
85.4	95.1	152.2	105.7	213.7	112.7	380.0	140.8	412.6	139.5	445.1	141.0
90.6	97.2	157.3	105.8	216.7	112.6	382.0	139.5	412.6	139.6	453.2	140.2
93.6	96.7	159.4	104.5	218.8	112.8	387.1	140.0	420.7	140.0		
95.7	97.0	162.4	106.5	223.9	114.0						
100.8	99.1	167.6	106.5	224.9	114.2				$RbNO_3$		
106.0	99.7	167.6	107.4	229.0	114.9						
110.1	98.7	172.7	107.6	233.1	116.0	60.7	108.1	93.6	115.5	126.5	120.5
111.1	99.2	175.8	108.3	234.1	115.2	64.8	110.9	95.7	116.4	134.7	120.2
116.2	99.8	177.8	107.9	239.2	116.2	69.0	111.6	106.0	117.7	136.8	122.3
118.3	99.3	182.9	110.0	241.3	118.9	70.0	110.3	110.1	118.2	141.9	122.0
121.4	102.7	184.0	108.2	244.3	120.0	75.1	112.4	111.1	119.9	147.0	128.8
126.5	102.5	188.1	108.8			77.2	110.6	116.2	118.4	151.1	124.2
		Solid-Liquid transition				80.3	113.7	118.3	118.3	152.2	127.7
275.0	141.4	315.8	141.3	356.6	140.8	85.4	112.5	121.4	119.5	157.3	127.6
280.1	141.8	320.9	141.6	361.7	140.5	90.6	114.0	126.5	120.1	159.4	127.7
282.2	140.3	326.0	141.3	366.8	140.9			Phase transition I			
285.2	140.8	331.1	139.3	371.9	141.4	198.3	149.8	208.5	151.9	216.7	151.5
290.3	139.3	331.1	139.7	377.0	140.5	200.3	153.7	208.5	152.1	218.8	153.5
290.3	140.5	336.2	141.0	382.0	140.0	203.4	149.1	213.7	154.3		
295.4	141.4	339.3	140.7	387.1	141.6			Phase transition II			
298.5	138.9	341.3	141.3	392.2	140.7						
300.5	140.7	346.4	140.5	397.3	141.1	254.6	149.0	264.8	148.8	275.0	153.2
305.6	140.5	347.4	138.9	402.4	140.3	257.6	150.4	265.8	148.5	280.1	160.8
310.7	140.9	351.5	141.6			259.7	147.2	274.0	153.8	282.2	160.0
314.8	140.1	355.6	139.1					Phase transition III			
			$NaNO_3$			300.5	156.6				
								Solid-Liquid transition			
59.7	98.9	90.6	104.1	126.5	111.0						
60.7	100.6	95.7	105.9	131.7	112.6	326.0	145.9	366.8	147.0	412.6	145.6
64.8	100.9	100.8	106.3	134.7	114.4	331.1	146.3	371.9	145.1	417.6	145.3
69.0	100.8	101.9	107.8	136.8	114.3	336.2	146.9	371.9	146.8	420.7	145.9
70.0	100.1	106.0	106.5	141.9	115.1	339.3	146.9	377.0	144.7	427.8	145.7
75.1	101.4	110.1	108.9	142.9	116.2	341.3	147.9	380.0	146.9	428.8	146.2
77.2	102.7	111.1	108.8	147.0	116.1	346.4	145.1	382.0	147.6	436.9	144.8
80.3	102.9	116.2	108.6	151.1	117.8	347.4	146.2	387.1	145.4	438.0	145.1
85.4	101.9	118.3	110.6	152.2	117.6	351.5	146.8	392.2	144.5	445.1	146.0
85.4	103.7	121.4	110.5	157.3	117.7	355.6	146.3	397.3	146.9	453.2	145.1
159.4	118.5	184.0	126.2	208.5	135.5	356.7	147.9	404.4	146.2	453.2	144.7
162.4	121.0	188.1	126.5	208.5	136.7	361.7	146.0	407.5	146.0		
167.6	122.1	192.2	128.8	213.7	137.1	363.7	146.8	412.6	144.4		
162.6	122.7	193.2	130.2	216.7	139.2				$CsNO_3$		
175.8	125.2	198.3	130.9	218.8	141.3						
177.8	125.3	200.3	132.2	223.9	142.3	64.8	108.2	95.7	111.5	131.7	124.0
182.9	126.4	203.4	133.4			69.0	109.9	101.9	111.9	134.7	119.5
		Phase transition				70.0	106.0	106.0	114.6	136.8	120.1
298.5	139.1	300.5	141.1	305.6	138.8	75.1	110.1	110.1	114.2	141.9	124.7
		Solid-Liquid transition				77.2	113.1	111.1	114.2	142.9	121.4
331.1	140.0	347.4	139.8	371.9	139.7	80.3	111.5	116.2	117.9	147.0	125.5
331.1	139.9	351.5	139.3	377.0	138.6	85.4	111.1	118.3	115.6	151.1	125.5
336.2	138.5	355.6	138.5	380.0	138.5	85.4	110.9	121.4	119.5	152.2	128.5
339.3	139.9	361.7	138.6	396.3	138.6	90.6	109.9	126.5	116.6		
341.3	138.7	363.7	139.1	397.3	138.7	93.6	111.5	126.5	117.9		
346.4	139.2	366.8	138.5	402.4	139.0			Phase transition			
			KNO_3			177.8	142.9	257.6	147.0	331.2	148.1
						182.9	143.1	259.7	147.7	336.2	149.1
						184.0	143.3	264.8	146.4	339.3	147.9
54.6	101.2	77.2	102.1	106.0	109.3	188.1	140.9	265.8	147.7	341.3	147.7
59.7	99.7	85.4	103.2	110.1	107.0	192.2	141.2	269.9	148.7	346.4	147.4
60.7	101.9	85.4	103.9	111.1	110.4	193.2	143.1	274.0	147.4	347.4	148.1
64.8	100.6	93.6	105.2	116.2	109.1	198.3	142.3	275.0	148.9	351.5	149.1
69.0	101.9	95.7	106.9	118.3	109.2	200.3	141.5	280.1	147.7	355.6	147.4
70.0	101.5	100.8	107.0	126.5	110.9	203.4	143.3	282.2	147.9	356.6	146.8
75.1	103.0	101.9	106.6			208.5	145.4	285.2	147.9	361.7	147.9
		Phase transition				208.5	144.0	290.3	147.7	363.7	147.7
159.4	128.4	218.8	129.3	269.9	133.4	213.7	143.5	290.3	149.3	366.8	147.7
162.4	131.5	223.9	129.9	274.0	136.3	216.7	143.5	295.4	149.1	371.9	148.3
167.6	128.7	224.9	128.8	275.0	134.7	218.8	145.8	298.5	147.7	371.9	147.4
167.6	126.0	229.0	130.9	280.1	135.5	224.9	144.6	300.5	149.3	377.0	147.9
172.7	127.0	233.1	131.3	285.2	136.0	229.0	147.2	305.6	148.9	380.0	148.1
175.8	127.7	234.1	129.9	290.3	136.1	233.1	145.6	306.6	148.5	382.0	145.8
177.8	126.8	239.2	130.2	295.4	137.1	234.1	146.6	310.7	148.3	387.1	147.6
182.9	127.6	241.3	132.4	298.5	138.7	139.2	145.8	314.8	149.3	388.1	146.6
184.0	127.0	244.3	131.6	300.5	137.8	241.3	147.0	315.8	147.9	392.2	147.9
188.1	127.5	249.5	131.4	305.6	139.0	244.3	145.0	320.9	149.3	396.3	147.7
192.2	127.4	249.5	132.5	306.6	138.4	249.5	147.4	323.0	147.2	397.3	146.8
198.3	128.2	254.6	130.9	310.7	138.5	249.5	147.2	326.0	148.1	402.4	146.2
200.3	127.6	257.6	132.9	314.8	140.1	254.6	147.6	331.1	147.6	404.4	147.4
208.5	128.7	259.7	134.0	315.8	140.7			Solid-Liquid transition			
213.7	128.2	264.8	133.1	320.9	139.1	432.9	143.9	443.0	141.7	448.1	141.1
216.7	129.6	265.8	132.7	323.0	140.4	436.9	142.5	445.1	142.7	453.2	142.7
						438.0	141.7				

t_{mp}. In comparison with the former our data are larger by *ca.* 23% for $LiNO_3$, smaller by *ca.* 10% for $NaNO_3$ and equivalent in magnitude for KNO_3; in comparison with the latter, our data are smaller by *ca.* 12% for $NaNO_3$ and larger *ca.* 12% for KNO_3. The temperature coefficients of C_p below t_{mp} are quite different between the previously reported data (*i.e.*, Barin and Knacke,[15] Goodwin and Kalmus,[1] Schüller,[8] and Regnault,[6]) and our data for $NaNO_3$ and KNO_3. It may thus be concluded that the reli-

ability of the literature data above t_{mp} is satisfactory only in the cases of Sokolov and Schmidt, and Carling. We had better say that the thermodynamic values of Gibbs free energy tabulated by Barin and Knacke are sufficiently accurate.

$LiNO_3$: Above 150 °C no satisfactory results were previously obtained.[1,21] No broad peaks associated with the reversible solid-state transition have been observed in the C_p measurements with an increase in the temperature. The substance of $LiNO_3$ is unique among the other alkali-nitrates because the difference $\Delta C_p^\circ(t_{mp})$ is not zero: $\Delta C_p^\circ(t_{mp})=23.2\,J\,K^{-1}\,mol^{-1}$, and no reversible solid-state transition takes place.

$RbNO_3$: To our knowledge, the only existing data on C_p are the data measured by Mustajoki.[19] The three reversible thermal transitions below t_{mp} and the solid-liquid transition are shown in Fig. 5. The data of Mustajoki above the first solid-phase transition temperature, which varies with the authors (*e.g.*, 160 °C was reported by Mustajoki while it is 166.3 °C in this work), are larger than ours by *ca.* 11%, as in the system of $NaNO_3$. The value of $\Delta C_p^\circ(t_{mp})$ may be slightly negative or almost zero, though it can not be estimated with accuracy because of the phase transition immediately below t_{mp}; the value reported by Mustajoki[19] is $-14.2\,J\,K^{-1}\,mol^{-1}$.

$CsNO_3$: The data of this work agree satisfactorily with the data by Sato[22] (see the dashed line in Fig. 6 between 0 and 100 °C but these temperatures are located below t_{tr}). The data of Mustajoki[20] and Flotow *et al.*[23] above 300 °C are larger than ours by less than *ca.* 19%. The values of t_{tr} and t_{mp} (*i.e.*, 151.5 °C and 405.5 °C, and 152 °C and 406 °C as reported by Mustajoki and by Flotow *et al.*, respectively) are rather low compared with ours (*i.e.*, 157.2 °C and 411.7 °C, which lie below each of the data in the other literature), as is shown in Fig. 6. The experimental values of C_p reported by Flotow *et al.* increase linearly with an increase in the temperatures over the entire temperature range above t_{tr}, except for the neighborhood of t_{mp}. Our data show that the heat capacities in the liquid state are almost independent of temperature for all the alkali metal nitrates. The C_p values below t_{tr} in the Flotow *et al.* data are smaller than ours and Mustajoki's. The value of $\Delta C_p^\circ(t_{mp})$ measured by Mustajoki depends on the systems, *i.e.*, $15.0\,J\,K^{-1}\,mol^{-1}$ for $NaNO_3$, -14.2 for $RbNO_3$ and *ca.* 0 for $CsNO_3$; in this work $\Delta C_p^\circ(t_{mp})=0\,J\,K^{-1}\,mol^{-1}$ for all the alkali metal nitrates which show a reversible solid-state transition. The values of t_{tr} and t_{mp} determined in this work are given by the figures in parentheses. The literature values are shown by the vertical lines in Figs. 2—6.

Some empirical rules which are possibly suitable for other typical salts have been obtained from the experimental results of C_p for the five alkali metal nitrates:

(1) The $\Delta C_p^\circ(t_{mp})$ defined in Eq. 2 is almost zero for MNO_3 accompanying the reversible solid-state transitions, *i.e.*, $NaNO_3$, KNO_3, $RbNO_3$, or $CsNO_3$.

(2) The heat capacities are independent of the temperatures above t_{mp} for all the nitrates. They increase linearly with an increase in the temperature until the first phase-transition temperatures (*i.e.*, $1.8\times10^{-3}\,J\,K^{-2}\,g^{-1}$ between 50 and 230 °C for $LiNO_3$, 2.3×10^{-3} between 50 and 150 °C for $NaNO_3$, 1.5×10^{-3} between 50 and 125 °C for KNO_3, 1.2×10^{-3} between 50 and 150 °C for $RbNO_3$, and 1.0×10^{-3} between 50 and 150 °C for $CsNO_3$); according to Southard and Nelson,[9] whose data near room temperature are shown by ★ in Figs. 3 and 4, the temperature coefficients of C_p for $NaNO_3$ and KNO_3 over the 100 °C range below room temperature are $2.1\times10^{-3}\,J\,K^{-2}\,g^{-1}$ and 1.5×10^{-3}, respectively. Therefore, between -100 °C and 150 °C the C_p values of $NaNO_3$ and KNO_3 increases linearly with an increase in the temperatures.

(3) Roughly speaking, the magnitude of the discontinuity, ΔC_p^{app}, at the temperature, t_p, corresponding to the maximum value of C_p is in inverse proportion to the thermal expansion α_T for the molten MNO_3 systems except for $RbNO_3$, which has three phase transition points below t_{mp}.

(4) Each of the $NaNO_3$, KNO_3, and $RbNO_3$ systems has nearly the same magnitude of enthalpy required for all the reversible solid-transitions, though the profile of C_p at t_{tr} and the number of the transitions below t_{mp} are dependent on the specific substances.

We shall confine our attention here to the heat capacities of MNO_3 in the liquid state. Starting from a formula for the difference between C_p and C_V, one obtains

$$\frac{C_p}{C_V}-1=\frac{u^2\alpha_T^2MT}{C_p} \tag{3}$$

or:

$$C_p-C_V=\frac{\alpha_T^2v_mT}{\beta_T}, \tag{4}$$

where u, α_T, M, v_m, and β_T are the sound velocity, the thermal expansivity, the molar weight, the molar volume and the isothermal compressibility, respectively.[24] Equation 3 or 4 is useful because we can determine C_V directly from the measured values of C_p and u or β_T. The values of C_V at $1.1\times T_{mp}$ are listed in Table 2, together with the data of β_T, u, α_T, and v_m. The magnitudes of C_V obtained from the compressibility data[25,26] are slightly larger than the C_V values obtained from the velocity data,[27-29] for the molten $CsNO_3$ or $RbNO_3$ with a large molar volume, as is shown in Table 2. No substantial difference between the values of C_V determined using the ultrasonic velocity data[27] and using the hypersonic velocity data[28,29] was found for fused $LiNO_3$ and $NaNO_3$. It is very interesting that the γ ratio, which is defined as C_p/C_V or β_T/β_s (β_s: adiabatic compressibility), increases roughly with an increase in the molar volume, v_m, among the five alkali-metal nitrates in the liquid state. The heat capacity C_V at a constant volume for the MNO_3 melts, consisting of monatomic univalent cations, M^+, and complex univalent anions, NO_3^-, can be divided into the interionic and intraionic portions:

$$C_V=C_V^{inter}+C_V^{intra}, \tag{5}$$

where C_V^{inter} is the sum of the contributions from the translation and configuration for both M^+ and NO_3^- ions and where C_V^{inter} is constructed of vibrational,

TABLE 2. HEAT CAPACITY AT A CONSTANT PRESSURE OR VOLUME OF MOLTEN ALKALI-METAL NITRATES

Sample	$T(=1.1\times T_m)$ K	$10^{11}\beta_T$[a] $N\,m^{-2}$	u[b] ms^{-1}	$10^4\alpha_T$[2] K^{-1}	$10^6 v_m$ m^3	C_p[c] $J\,K^{-1}\,mol^{-1}$		C_V[d] $N_A k_B$	γ	10^3 M kg	t_{mp}[c] °C
$LiNO_3$	582.7	18.1[25]	—	2.88	36.6			15.7	1.08	68.95	256.5
		20.0[26]	—			140.6	+1.2	15.9	1.07		
		—	1783[27]				−1.7	15.7	1.08		
		—	1751[28]					15.8	1.07		
$NaNO_3$	641.7	19.8[25]	—	3.46	41.3			14.8	1.13	85.01	310.2
		19.6[26]	—					14.8	1.13		
		—	1740[27]			139.1	+0.9	14.6	1.15		
		—	1761[28]				−0.6	14.6	1.15		
		—	1762[29]					14.6	1.15		
KNO_3	670.5	22.4[25]	—	3.60	49.9			15.2	1.11	101.1	336.3
		22.7[26]	—					15.2	1.11		
		—	1683[27]			140.3	+1.3	15.3	1.10		
		—	1766[28]				−1.4	14.8	1.14		
		—	1751[29]					14.8	1.14		
$RbNO_3$	645.4	23.5[25]	—	3.62	54.9			15.2	1.16	147.49	313.5
		20.9[26]	—			146.0	+1.9	14.9	1.18		
		—	1506[28]				−1.6	14.7	1.19		
$CsNO_3$	753.4	33.6[25]	—	3.81	63.7			14.6	1.17	194.92	411.7
		30.6[26]	—			142.3	+1.6	14.4	1.19		
		—	1198[28]				−1.2	14.1	1.21		

a) Obtained from the measurement of $(\partial T/\partial P)_s$ in 26) and from the p-V-T studies in 25). b) Hypersonic velocities in 28) and 29), and ultrasonic velocities in 27). c) This work. d) Obtained using Eq. 3 or 4.

rotational and electronic parts in the NO_3^- ion.[30] The values of $C_V^{vib}/N_A k_B$ and $C_V^{rot}/N_A k_B$ are 6 and 1.5 respectively, in accord with the classical theory of the heat capacity of an assembly of independent, rigid, non-linear molecules for NO_3^- ions.[30]

Under the assumption of a point charge model for the univalent melts, the C_V^{trans}, C_V^{config}, and C_V^{elec} values of the molten MNO_3 are equal to 3, 3, and 0 respectively in units of $N_A k_B$. The estimated value of $C_V/N_A k_B$, 13.5, should be compared with the results of the $C_V/N_A k_B$ values of the five molten MNO_3 at $1.1\times T_{mp}$ cited in Table 2, in which the disagreement may originate mainly from the short estimation of C_V^{config} for molten MNO_3. The molten alkali nitrates have a higher heat capacity (*i.e.*, *ca.* $15\times N_A k_B$) at a constant volume than that (*ca.* $6.0\times N_A k_B$) of molten alkali chlorides because of the vibrational and rotational contributions associated with NO_3^-. The hard-sphere models[31,32] applied to the thermodynamic properties of simple molten salts are not adequate for the molten nitrates which consist of complex anions, NO_3^-, and monatomic cations M^+.

Once again let us focus on the difference, ΔC_p^{app}, between the maximum value of C_p near t_{mp} and the value of C_p corresponding to the horizontal line linking the open circles shown in the upper part of Figs. 2—6. The ΔC_p^{app} quantity should not be confused with the $\Delta C_p^{\circ}(t_{mp})$ defined in Eq. 2 and should be infinite, though it is apparently finite in the experimental results. Such values of ΔC_p^{app} may originate from the sudden appearance of the communal entropy at the melting point because each ion can move anywhere in the liquid, whereas in the crystal the ions are localized systems.

Some of the techniques used have serious drawbacks, since some previously reported data on heat capacities in the liquid state are much too high, and their temperature coefficients are not certainly less than the positive values in the solid state.[34] The conclusion in this work is that the heat capacity of each molten alkali-metal nitrate is in the range from 138 to 148 $J\,K^{-1}\,mol^{-1}$ and is probably independent of the temperature. At this point, it should be possible to regard some sets of results above t_{mp} as better than others.

We wish to thank Professor Hideaki Kita for his encouragement during the course of this work. We also greatly appreciate the help of Professor G. J. Janz in supplying the sample of KNO_3 used in this work and for showing us a number of references on the heat capacities of ionic melts which were retrieved by the Molten Salt Data Center, Rensselaer Polytechnic Inst., USA. We also wish to thank Dr. D. K. Tödheide for his comments on the compressibility and velocity data of the molten nitrates. This work was supported by a Grant-in-Aid for Scientific Research No. 56470001 from the Ministry of Education, Science and Culture.

References

1) *E.g.* H. M. Goodwin and H. T. Kalmus, *Phys. Rev.*, **28**, 1 (1909).
2) G. J. Janz, "Molten Salts Handbook," Academic Press, New York (1967), p. 184.
3) W. W. Wendlandt, "Thermal Methods of Analysis," Interscience Pub., New York (1964), p. 132.

4) Y. S. Touloukian and C. Y. Ho, "Thermophysical Properties of Matter, Specific Heat (Vol. 4)," Heyden Pub., London.
5) N. Onodera, A. Kimoto, M. Sakiyama, and S. Seki, *Bull. Chem. Soc. Jpn.*, **44**, 1463 (1971).
6) H. V. Regnault, *Ann. Chim. Phys.*, **1**, 129 (1841).
7) C. C. Person, *Ann. Chim. Phys.*, **21**, 295 (1847).
8) J. H. Schüller, *Pogg. Ann.*, **136**, 70 and 235 (1869).
9) J. C. Southard and R. A. Nelson, *J. Am. Chem. Soc.*, **55**, 4865 (1933).
10) H. Miekk-Oja, *Ann. Acad. Sci. Fenn., Ser. A*, **1**, 7 (1941).
11) V. A. Sokolov and N. E. Schmidt, *Izv. Sekt. Fiz-Khim. Anal. Inst. Obsh. Neorg. Khim. Acad. Nauk. SSSR*, **26**, 123 (1955).
12) A. Mustajoki, *Ann. Acad. Sci. Fenn., Ser. A*, **6**, 5 (1957).
13) G. J. Janz, F. J. Kelly, and J. L. Perano, *J. Chem. Eng. Data*, **9**, 133 (1964).
14) V. C. Reinsborough and F. E. W. Wetmore, *Aust. J. Chem.*, **20**, 1 (1967).
15) I. Barin and O. Knacke, "Thermochemical Properties of Inorganic Substances," Springer-Verlag, Berlin (1973).
16) R. W. Carling, "Proc. of the Third Inter. Symp. on Molten Salts," ed by G. Mamantov, M. Blander, and G. P. Smith, Elect. Soc., Pennington (1981), p. 485.
17) V. A. Sokolov and N. E. Schmidt, *Izv. Fiz-Khim. Anal. Inst. Obsh. Neorg. Khim. Acad. Nauk. SSSR*, **27**, 217 (1956).
18) A Mustajoki, *Ann. Acad. Sci. Fenn., Ser. A*, **6**, 99 (1962).
19) A. Mustajoki, *Ann. Acad. Sci. Fenn., Ser. A*, **6**, 9 (1958).
20) A. Mustajoki, *Ann. Acad. Sci. Fenn., Ser. A*, **6**, 7 (1957).
21) "Landolt-Börnstein, Zahlenwerte und Funktionen, II. Band 4. Teil: Kalorische Zustandsgroβen," Springer-Verlag, Berlin (1961), p. 502.
22) S. J. Sato, *Sci. Res. Inst. Tokyo*, **48**, 59 (1954).
23) H. E. Flotow, P. A. G. O'Hare, and J. J. Boerio-Goates, *Chem. Thermodyn.*, **13**, 477 (1981).
24) E.g., K. S. Pitzer and L. Brewer, "Thermodynamics," McGraw-Hill, New York (1961), p. 102.
25) J. E. Bannard and A. F. M. Barton, *J. Chem. Soc., Faraday Trans. 1*, **74**, 153 (1978).
26) B. Cleaver and P. Zain, *High Temp.-High Pressures*, **10**, 437 (1978).
27) J. O'M. Bockris and N. E. Richards, *Proc. R. Soc. London, Ser. A*, **241**, 44 (1957).
28) H. E. G. Knape and L. M. J. Torell, *Chem. Phys.*, **62**, 4111 (1975).
29) T. Ejima, K. Shimakage, T. Yamamura, Y. Sato, T. Yoko, H. Nakatao, and Y. J. Kobayashi, *Jpn. Inst. Metals.*, **46**, 43 (1982).
30) E.g., G. S. Rushbrook, "Introduction to Statistical Mechanics," Clarendon Press, Oxford (1951), pp. 84 and 127.
31) H. Reiss, *Adv. Chem. Phys.*, **9**, 1 (1965).
32) T. Itami and M. Shimoji, *J. Chem. Soc., Faraday Trans. 2*, **76**, 1347 (1980).
33) C. N. R. Rao and K. J. Rao, "Phase Transitions in Solids," McGraw-Hill, New York (1978), p. 17.
34) E.g., P. Nguyen-Duy and E. A. Dancy, *Thermochim. Acta*, **39**, 95 (1980).